CdSe Quantum Dot-Sensitized TiO_2 Electrodes: Effect of Quantum Dot Coverage and Mode of Attachment

Néstor Guijarro,[†] Teresa Lana-Villarreal,[†,*] Iván Mora-Seró,[‡] Juan Bisquert,[‡] and Roberto Gómez[†,*]

Institut Universitari d'Electroquímica i Departament de Química Física, Apartat 99, E-03080 Alacant, Spain, and Departament de Física, Universitat Jaume I, Castelló, Spain

Received: September 11, 2008; Revised Manuscript Received: January 9, 2009

We have investigated the sensitization of nanoporous titanium dioxide by previously synthesized CdSe quantum dots (QDs) protected with trioctylphosphine. Covering the nanoporous TiO_2 films with QDs has been achieved using two strategies: (i) direct adsorption from dichoromethane dispersions and (ii) anchoring the QDs through a molecular linker, concretely, mercaptopropionic acid (MPA). In contrast with MPA-mediated adsorption, direct adsorption leads to a high degree of QD aggregation, as revealed by atomic force microscopy (AFM) images obtained with both TiO_2 nanoporous films and monocrystalline surfaces. Importantly, at saturation, only 14% of the real surface area of a 5-μm thick P25 TiO_2 layer is covered for both attachment modes. For MPA attachment, the incident photon-to-current efficiency (IPCE) increases with the loading, whereas a maximum (close to 40% at the QD excitonic peak) is defined for intermediate coverages in the case of QD direct adsorption. In addition, for equivalent QD loading, IPCE values are larger in the case of direct adsorption.

Introduction

Dye-sensitized solar cells based on mesoscopic wide band gap semiconductors have the potential advantages of lower cost production and versatility in comparison to the conventional solid-state cells.[1] The photoanode in such cells is constituted by a nanoporous TiO_2 layer sensitized to the visible radiation by an adsorbed dye. Instead of using dyes, the sensitization of TiO_2 nanoporous electrodes can be achieved through modification of the oxide with quantum dots (QDs) of low band gap semiconducting materials. The use of QDs enables band gap tuning through control of the QD size, which allows one to adjust both light absorption and the energetics at the interfaces of the QD with the surrounding media (hole and electron transporting materials). In addition, QD solar cells could benefit from both large QD extinction coefficients and the multiple exciton generation phenomenon, which should lead to an enhancement of the conversion efficiency in solar cells.[2,3] QDs thus have the potential to overcome the energy loss of highly energetic photons caused by carrier thermalization in conventional solar cells.

The initial works utilized different quantum-sized sulfides to sensitize TiO_2 nanoporous electrodes.[4,5] Many systems have been studied since then, like those based on the following QD sensitizers, in which cadmium chalcogenides play a central role: CdS,[4−10] PbS,[5,11−13] InP,[14] InAs,[15] CdSe,[16−25] and CdTe.[26] In the case of CdSe QDs, several aspects have been analyzed, such as cosensitization with a dye,[17] TiO_2 particle size and shape[21,23,24] and the influence of surface modification of the QDs with either fluoride or ZnS.[23,27] Very recently, the effect of the QD diameter has also been examined.[20] On the other hand, combining both CdSe QD sensitization and nitrogen doping of the TiO_2 matrix has been proposed as an effective and promising way to enhance the response of the photoanode.[28]

One of the subjects investigated recently is the type of attachment of the QDs to the oxide matrix. In fact, one of the reasons leading to the poor efficiency of QD-sensitized solar cells is the difficulty of linking the QDs to the mesoporous TiO_2 matrix to obtain a full monolayer on the TiO_2 surface. In most of the reported works, QDs were grown directly onto the nanoporous matrix by chemical bath deposition. Although a direct contact between the oxide and the QDs is achieved in this way, there is no separate control of QD coverage and size. In addition, the deposits could be far from stoichiometric because of, for instance, the possible formation of elemental layers in addition to the sought compound particles.

These drawbacks can be avoided if the QDs are synthesized previously, and, later, the oxide layer is modified with them.[14−16,20,25,26,28] In most cases, the attachment of the QDs to the oxide is achieved by using a linker, which is a bifunctional molecule that anchors the QD to the oxide particle, acting as a molecular cable. Different molecular linkers have been investigated, and it has been recognized that the chemical nature of the linker plays a decisive role in determining the efficiency of electron injection into the matrix. Kamat and co-workers reported that mercaptopropionic acid (MPA) is a better linker than thiolacetic or mercaptohexadecanoic acid.[20] In a similar way, we very recently showed that using cysteine as a linker gives rise to more efficient photoanodes than using thioglycolic acid or MPAs.[24] In this paper we compare the behavior of CdSe QD-sensitized TiO_2 electrodes in which the QDs are attached to the oxide either through the use of a linker, such as MPA, or by direct adsorption of the capped QDs. In each case, the dependence of the IPCE on the QD loading is analyzed. The deleterious effect of QD aggregation is evidenced.

Experimental Section

CdSe QDs, capped with trioctylphosphine (TOP), were prepared by a solvothermal route that permits size control.[29]

* Corresponding authors. E-mail: Roberto.Gomez@ua.es; Teresa.Lana@ua.es; fax: +34 965903537; phone: +34 965903536.
[†] Universitat d'Alacant.
[‡] Universitat Jaume I.

10.1021/jp808091d CCC: $40.75
Published on Web 02/16/2009

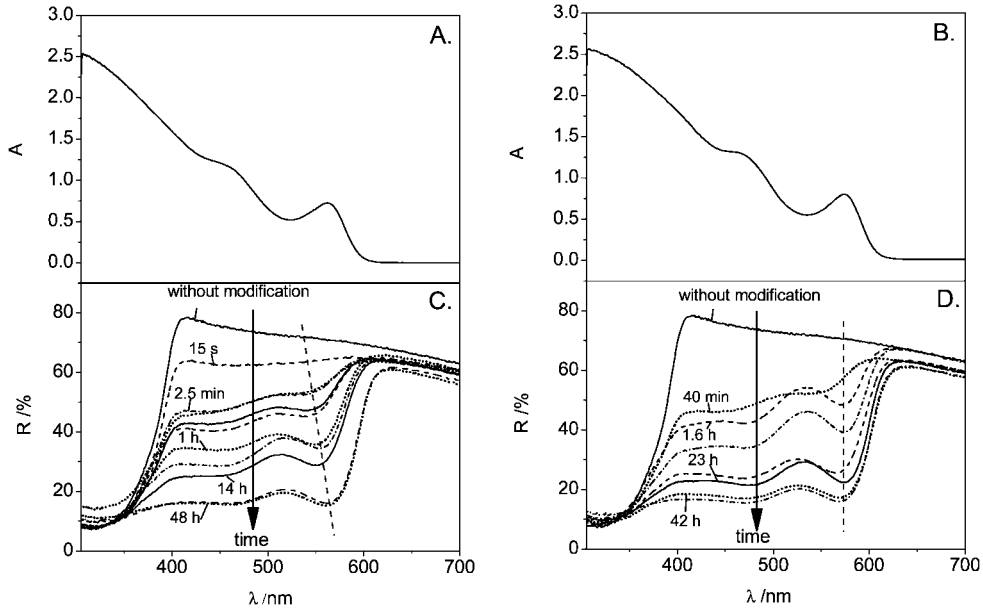

Figure 1. Absorption spectra of CdSe QD colloidal dispersions used for (A) direct and (B) MPA-mediated adsorption. Corresponding reflectance spectra of TiO_2 nanoporous films sensitized with CdSe QDs by direct adsorption (C) and using MPA as a linker (D) after different immersion periods in the corresponding solution. The arrow indicates increasing times.

Briefly, selenium (99.5%, Alfa Aesar) reacts with cadmium myristate in toluene (99.5+%, Sigma Aldrich) in the presence of oleic acid (~99%, Sigma Aldrich) and TOP (90%, Aldrich). The reaction takes place at 180 °C in a sealed autoclave. The reaction time allows to control the QD size and, consequently, the QD band gap. All the electrodes studied in the present work have been prepared with QDs of very similar size using a reaction time of 15 h. The as-prepared CdSe QDs were purified prior to their utilization by precipitation in ethanol, isolation by centrifugation, and decantation at least three times.

Nanoparticulate electrodes were prepared by spreading an aqueous slurry of Degussa P25 TiO_2 nanoparticles over 1.4 cm^2 of F:SnO_2-coated glass substrates. The suspension was prepared by grinding 1 g of TiO_2 powder with 1.8 mL of H_2O, 30 μL of acetylacetone (99+%, Aldrich) and 30 μL of Triton X100 (Aldrich). Typically 10 μL of this suspension was applied per substrate. Afterward, the films were annealed and sintered for 1 h at 450 °C in air. The resulting film thickness was ~5 μm as determined by scanning electron microscopy.

Two types of sensitized TiO_2 samples were prepared. In the case of direct QD adsorption, a CH_2Cl_2 (99.6%, Sigma Aldrich) CdSe QD dipersion was obtained by centrifugation of the toluene colloidal dispersion in the presence of ethanol, and redissolution. The TiO_2 electrodes were immersed in such a dispersion for times ranging between 15 s and 48 h. In the case of adsorption through a linker, nanoparticulate TiO_2 electrodes were modified with 3-MPA (99%, Aldrich) by inmersion in a 1:10 acetonitrile (99.5%, Sigma Aldrich) solution for 24 h. The electrodes were rinsed thoroughly with acetonitrile and immersed in toluene for 1/2 h, before being transferred to the toluene CdSe QD solution. The electrodes were left in such a solution for times ranging from 40 min to 42 h.

The absorption spectra were obtained with a Shimadzu UV-2401 PC. In the case of the diffuse reflectance spectra of sensitized TiO_2 electrodes, an integrating sphere was employed, using $BaSO_4$ (Wako) as background.

Photoelectrochemical measurements were performed at room temperature in a three-electrode cell equipped with a fused silica window using a computer-controlled Autolab PGSTAT30 potentiostat. All potentials were measured against and are referred to a Ag/AgCl/KCl(sat) reference electrode, whereas a Pt wire was used as a counter electrode. In all the experiments, a N_2-purged 0.5 M solution of Na_2SO_3 (98.0% min, Alfa Aesar) in ultrapure water (Millipore Elix 3) was used as the working electrolyte. A 150 W Xe arc lamp (Oriel) equipped with a monochromator (Oriel model 74000) was used for electrode illumination from the substrate side. The light intensity was measured with an optical power meter (Oriel model 70310) equipped with a photodetector (Thermo Oriel 71608).

The amount of deposited CdSe QDs was determined by inductively coupled plasma atomic emission spectrometry (Perkin-Elmer Optima 3000), by the dissolution of CdSe QDs in a 4% H_2O_2 (30%, Merck) solution containing 3% of HNO_3 (65%, p.a., Merck).

Atomic force microscopy (AFM) was performed using a Nanoscope III (Digital Instruments) operated at room temperature in air. Images were obtained in tapping mode using silicon tips at a driving frequency of ~270 kHz. n-Type rutile TiO_2(110) single crystals, doped with 0.075 wt % Nb_2O_5 were purchased from Commercial Crystal Laboratories, Inc. In order to define an atomically smooth surface, the single crystal was treated as described previously.[30] Once washed with acetone, it was immersed in 24% HF (48%, p.a., Merck) for 10 min and annealed at 550 °C for 3 h in air. The adsorption of QDs on the rutile single crystal samples was performed following the same experimental procedure as that for the nanoporous TiO_2 electrodes.

Results and Discussion

Figure 1A,B shows the absorption spectra corresponding to the CdSe QD dispersions used for direct and linker-mediated adsorption. It should be noted that, apparently, the sizes of the QDs in both dispersions are slightly different in spite of the fact that they were synthesized in the same way. These small differences are attributed to variations inherent to the synthetic method. In any case, both dispersions are characterized by a well-defined peak at 560−570 nm (1st excitonic peak), which reveals a narrow size (diameter) distribution around 3.4 ± 0.1

nm.[31] The modification of the TiO_2 nanoporous layer, for both direct and linker-mediated attachment, results in the development of a deep reddish coloration, which attests to a high degree of QD attachment to the TiO_2 nanoporous layer. In Figure 1C,D, series of diffuse reflectance spectra obtained for different immersion times of the nanoporous thin film in the corresponding QD dispersion are shown. Diffuse reflectance instead of absorbance is presented because of light scattering. In order to make their comparison with the absorbance spectra of the QD dispersions more straightforward, the reflectance spectra were subjected to the Kubelka−Munk transformation and are shown in Figure S1 (see Supporting Information). The uppermost spectra in Figure 1C,D correspond to the unmodified TiO_2 film and are characterized by a sharp drop of the reflectance at 400 nm, that is, at the wavelength corresponding to the TiO_2 band gap. Upon the introduction of the QDs, there is an important decrease in the reflectance in the visible region below 600 nm, due to QD absorption. It is remarkable that all the spectra show either a shoulder or a minimum for the wavelengths corresponding to the CdSe QD excitonic peak.

Close inspection of both series reveals a difference between them. Whereas the excitonic peak in the case of MPA-mediated adsorption is located at a constant wavelegth, it seems to slightly shift (by as much as 20 nm) toward longer wavelengths as the QD coverage increases in the case of direct adsorption (see also Figure S1). Interestingly, this points to a certain degree of QD aggregation in the latter case. The magnitude of the shift observed in Figure 1C (and also in Figure S1C) as the QD coverage increases is similar to that found for films of CdSe QDs of similar size upon strong aggregation after drying.[32] In addition, incorporation of the QDs (at low coverage) into the TiO_2 matrix causes a blueshift of the corresponding spectra as large as 20 nm. A similar effect has been observed in the case of cyanide adsorption on nanoparticulate CdSe films,[32] being attributed to the electrostatic compression of the localized excited electron by the negatively charged, strongly adsorbed cyanide. We believe that, in our case, the observed behavior is related to important structural and environmental changes occurring upon QD adsorption at the TiO_2 surface. On the one hand, adsorption triggers a change in the effective dielectric constant external to the QD. On the other, it is likely that by direct QD adsorption there is a partial removal of the TOP layer. In fact, the effect on the QD absorption spectra of the dielectric constant of the medium surrounding the QDs has been analyzed in detail both theoretically and experimentally.[33] In addition, small shifts of the excitonic peak as a result of ligand exchange have also been described.[34]

Achieving an effective coverage of the oxide with the QDs is a major issue for the improvement of this type of QD solar cell.[24] To obtain a quantitative assessment of the amount of adsorbed QDs, they were dissolved in an acidic oxidant solution containing nitric acid and hydrogen peroxide, and the total amount of cadmium was determined by atomic emission spectrometry. As expected, this amount correlates well with 100-R% (see Supporting Information, Figure S2). The saturation amount of Cd after 48 h corresponds to 60 $\mu g/cm^2$ of projected (geometric) electrode area for both anchoring methods. This cadmium mass corresponds to a particle concentration equal to 8.5×10^{14} cm^{-2}, if we consider them as spherical and monodispersed with a diameter of 3.4 nm. On the basis of a closed packed QD monolayer, the total surface area covered by the particles would be of 85 cm^2. On the other hand, the Degussa P25 powder used for making the thin film electrodes has a Brunauer−Emmett−Teller (BET) surface area of 51 $m^2 \cdot g^{-1}$.[35] We determined gravimetrically the weight of the 5 μm-thick film, obtaining a value of 1.15 $mg \cdot cm^{-2}$, which means that 45% of the thin film volume corresponds to pores. Therefore, the total inner surface area of the film is as large as 590 cm^2/cm^2 of projected area. Finally, by dividing the surface area that may be covered by the CdSe QDs by the total surface area of the oxide, we find a value for the QD fractional coverage equal to 0.14. This result highlights the fact that only a small fraction of the pores is accessible to the QDs. In this connection, it should be mentioned that direct adsorption is initially much faster than MPA-mediated adsorption (compare the adsorption times in Figures 1C,D), suggesting QD accumulation on top of the TiO_2 layer.

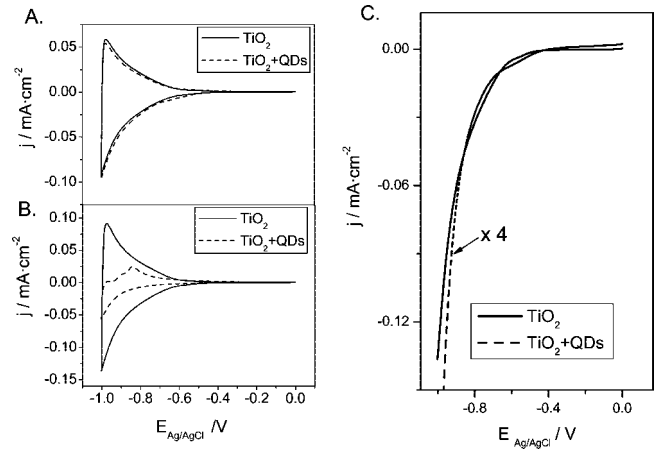

Figure 2. Cyclic voltammograms for TiO_2 nanoporous electrodes before and after sensitization through direct adsorption of CdSe QDs after (A) several minutes and (B) after 48 h, in N_2 purged aqueous 0.5 M Na_2SO_3. Scan rate, 20 $mV \cdot s^{-1}$. (C) Comparison between the voltammetric profiles before and after direct adsorption of CdSe QDs for 48 h. The current for the sensitized electrode has been multiplied by a factor of 4.

It should be stressed that direct adsorption does not occur when the TOP-capped QDs are dispersed in toluene. This result points to the fact that the adsorption behavior of QDs at porous TiO_2 films is rather sensitive to experimental conditions, particularly to the solvent used for the QD dispersions. Understandably, the driving force for direct QD adsorption on TiO_2 is small, being important to tune the interactions among colloids, solvent, and surface. In a very recent report, Lee at al[36] also found that direct adsorption of TOPO-capped CdSe QDs on TiO_2 nanoporous films barely occurs when dispersed in toluene.

Figure 2 shows dark voltammetric profiles obtained in aqueous 0.5 M Na_2SO_3 for TiO_2 electrodes modified with CdSe QDs through direct adsorption. As observed, the profiles are dominated in all cases by the chemical capacitance typical of nanoporous TiO_2 films for potentials lower than -0.5 $V_{Ag/AgCl}$. Such voltammetric responses (in the negative-going scan) are usually interpreted as the filling, with electrons coming from the substrate, of an exponential distribution of trap states below the conduction band.[37,38] In addition, some of us have recently suggested on the basis of experimental results that these capacitive currents are proportional to the interfacial (electrochemically active) area.[39] The negative charge accumulated in the nanocrystalline layer during the cathodic scan needs to be compensated with species coming from the electrolyte, protons, or sodium cations, mainly through adsorption, although hydrogen insertion into the TiO_2 nanoparticles cannot be discarded. When the CdSe adsorption times are in the range of minutes (Figure 2A), the capacitive current of the nanoporous matrix

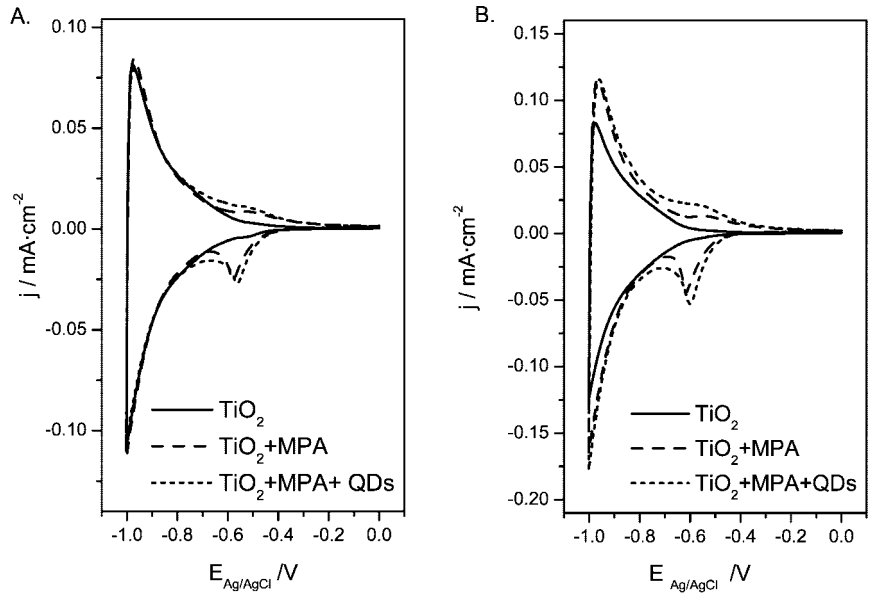

Figure 3. Cyclic voltammogram for TiO_2 nanoporous electrodes before and after anchoring CdSe QDs through MPA after (A) 40 min and (B) after 42 h, in N_2 purged aqueous 0.5 M Na_2SO_3. Scan rate 20 $mV \cdot s^{-1}$.

remains practically unaltered. However, for adsorption times in the range of hours (Figure 2B), the presence of QDs leads to a drastic decrease of the capacitance, which can be interpreted as resulting from the impeded access of the cations to the oxide surface. Part of the interfacial area would be blocked due to QD accumulation in the outer part of the TiO_2 film leading to a decreased capacity. Alternatively, one could argue that there is a shift of the conduction band edge toward more negative electrode potentials (higher potential energies) due to an equilibration process between the QD and TiO_2 bands. Nevertheless, when the negative-going scan is multiplied by a factor of 4, the resulting curve is rather similar to that corresponding to the bare TiO_2 electrode (Figure 2C). This is a good indication of the same energetic location for the surface/conduction band states, although with a remarkable lower apparent density of states when the QDs are present, which we interpret as a decrease of the effective TiO_2 volume contributing to the capacitance.

In the case of the MPA-mediated adsorption, the situation is rather different. Figure 3 shows the cyclic voltammograms resulting from the modification of the TiO_2 nanocrystalline layer with MPA and from the subsequent attachment of the QDs via the MPA linker. As observed, in both cases, minor changes in the profile are observed, but the overall capacitance of the electrode is not altered in an important way regardless of the amount of QDs attached to the oxide matrix. This behavior suggests that the oxide surface can be easily accessed by the ions of the electrolyte, the capacitance not varying in a significant way. In addition, the adsorption of MPA gives rise to the appearance of a small peak at -0.62 V, probably linked to the filling of traps or surface states caused by the adsorption of MPA.[40] A minor shift (around 30 mV) of the capacity curve toward more positive potentials is often observed. This fact points to a shift of the TiO_2 conduction band edge toward lower energies. The ability of some adsorbents to move the conduction band of nanoporous TiO_2 films has been described in the context of dye-sensitized solar cell research.[41−43] A downward shift of the TiO_2 bands can result from a partial removal of the negative charge density typical of the TiO_2 surface at the pH of the electrolyte or to an alteration in the solvent structure in the interphase caused by the presence of the adsorbate. Importantly, such a behavior is observed prior to QD attachment, indicating that the possible band edge shift is not related to interactions between TiO_2 and CdSe particles.

The different voltammetric behavior shown by the CdSe/TiO_2 electrodes prepared either by direct adsorption or with the MPA linker is probably related to a different distribution of the QDs in the nanoporous layer. In the case of direct adsorption, the affinity of the dispersed QDs for already adsorbed ones may be similar to their affinity for the bare oxide surface. This would favor the aggregation of the QDs, particularly in the outer part of the TiO_2 film, at the entrance of the nanochannels, which probably underlies a faster initial QD adsorption. The bottlenecks formed because of aggregation would hinder the access of the electrolyte deep into the pores, leading to a decrease of the effective electrochemical active area of the substrate, particularly taking into account the hydrophobic character of the TOP chains. Conversely, in the case of a TiO_2 surface modified with MPA, anchoring the QDs to the oxide surface is favored because of the very strong interaction between the thiol group and the CdSe surface. Probably, each QD would be linked to the oxide surface by means of several MPA molecular cables. This would render the interaction of QDs with the modified oxide surface more favorable than that with previously adsorbed QDs, preventing in such a way the tendency to aggregation. As mentioned above, direct adsorption from a toluene QD dispersion scarcely occurs on a bare TiO_2 porous film. However, we cannot entirely rule out the possibility of aggregation in the case of MPA-mediated adsorption.

To study the eventual aggregation process occurring during TiO_2 modification with QDs, tapping-mode AFM images were obtained for different samples. Figure 4A shows the characteristic morphology of a P25 TiO_2 porous film. After anchoring CdSe QDs via MPA, a similar morphology is observed, that is, a nanostructure composed of well-defined particles (figure 4B). In the case of the direct CdSe QD adsorption the AFM image is blurry, less well-defined (figure 4C). In addition, very different particle sizes can be observed, the smallest being about 6−7 nm (Figure 4D). These particles can be identified as the CdSe QDs. It should be remarked that the average diameter estimated from the excitonic peak is smaller (3.4 ± 0.1 nm) than the one estimated from the AFM images. The different particle size

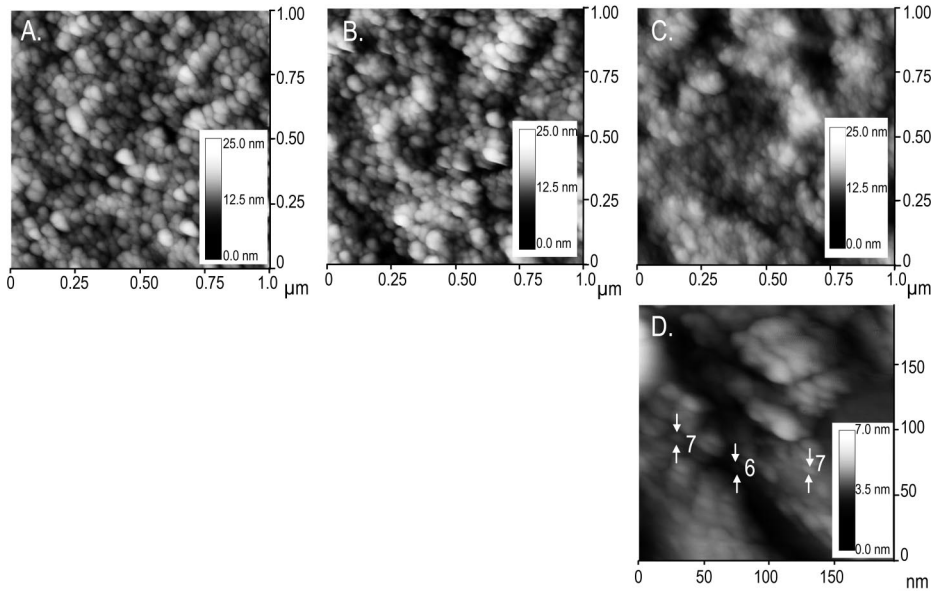

Figure 4. Tapping-mode AFM images for (A) a bare TiO_2 P25 nanoporous thin film, (B) a nanoporous TiO_2 film with CdSe QDs anchored through MPA and (C,D) a nanoporous TiO_2 film with directly adsorbed CdSe QDs.

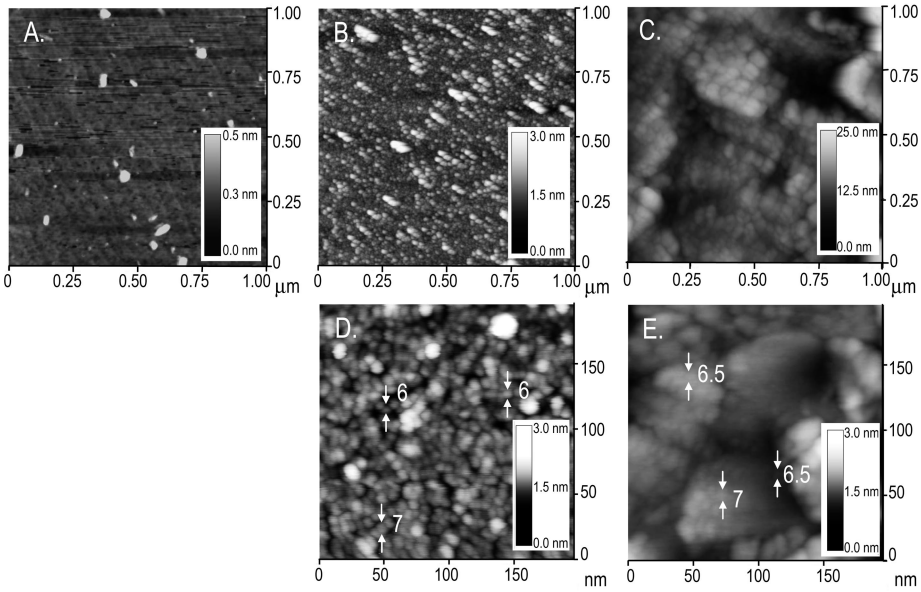

Figure 5. Tapping-mode AFM images of (A) a bare Nb-doped (110) rutile single crystal, (B,D) a single crystal with CdSe QDs anchored through MPA and (C,E) a single crystal with directly adsorbed CdSe QDs.

obtained from both methods is probably caused by the capping agent (TOP), which is supposed to give a larger particle size of CdSe when observed by tapping-mode AFM. However, it should also be noted that, in AFM images, the size of small particles tends to be overestimated.

Because of the difficulties in imaging the QD distribution when adsorbed at the nanoporous TiO_2 film, (110) niobium-doped TiO_2 single crystals were used as substrates to incorporate the QDs using both assembling methods. In Figure 5A, the smooth surface morphology of the TiO_2 single crystal is evidenced with terraces and monatomic steps (together with some large clusters). The crystal was then modified with MPA and immersed in the QD dispersion. Times were chosen as to allow for saturation. The corresponding AFM images are shown in Figure 5B,D. A nearly close packed layer of QDs can be observed on top of the single crystal surface. Most of these nanoparticles are in the range of 6 to 7 nm (Figure 5D), corresponding to the apparent size of CdSe QDs capped with TOP. However, a few larger clusters can also be observed, which indicates a small tendency to aggregation and/or formation of a bilayer.

After 48 h of CdSe QD direct adsorption from a CH_2Cl_2 dispersion, the AFM images shown in Figure 5C,E were obtained. The surface appears now as highly roughened and is composed, for the most part, of clusters larger than the size of a single QD, indicating a high degree of QD aggregation. However, in some areas, individual CdSe QDs can also be observed (Figure 5E). The AFM images obtained for niobium-doped (110) rutile are thus consistent with previous results obtained for P25 nanoporous electrodes.

The effectiveness of the $CdSe/TiO_2$ electrodes as photoanodes in photoelectrochemical QD-sensitized solar cells has been assessed by incident photon-to-current efficiency (IPCE) measurements in a standard three electrode electrochemical cell. The sulfite solution used for the electrochemical characterization in the dark was also employed for the IPCE measurements

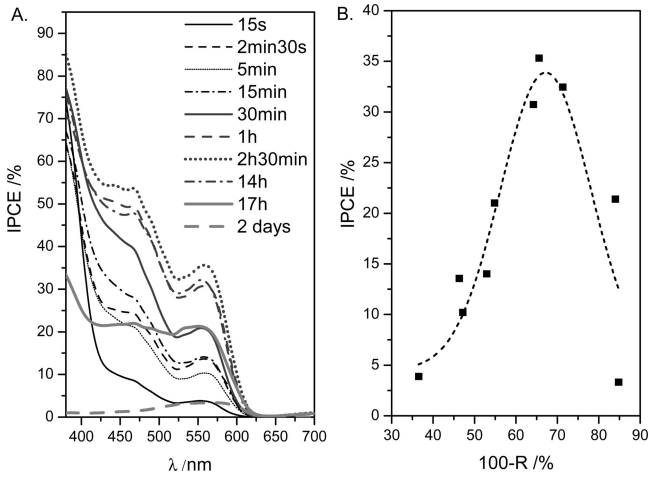

Figure 6. (A) IPCE spectra of TiO_2 nanoporous electrodes sensitized through direct adsorption of CdSe QDs with different coverage values. (B) IPCE at the excitonic peak vs 100-R % at the excitonic peak.

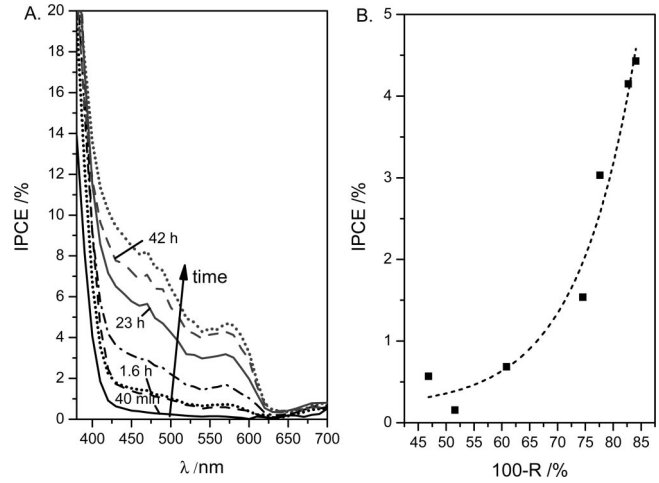

Figure 7. (A) IPCE spectra of TiO_2 nanoporous electrodes sensitized with MPA-attached CdSe QDs at different coverage values. (B) IPCE at the excitonic peak vs 100-R % at the excitonic peak.

because it is an efficient hole scavenger.[7] It is important to mention that no apparent photocurrent instability or electrolyte diffusion limitations were observed during the experimental measurements. Figure 6A shows the IPCE vs incident wavelength curves for different QD coverages in the case of direct adsorption. As observed, the IPCE spectra adhere well to the shape of the absorption spectrum of the QDs dispersed in toluene (Figure 1A) being also distinguishable the first excitonic peak. As the QD coverage increases, the IPCE first increases and then decreases, attaining a very low value for an adsorption time of two days (Figure 6B). This means that, in the latter case, most of the photogenerated carriers recombine. Probably, such an enhanced recombination is connected to the fact that aggregation of the QDs leads to the generation of excitons in QDs not in direct contact with the oxide. Since the extraction of electrons to the adjacent medium does not occur, recombination is enhanced. This loss has been suggested to be caused when electrons have to cross semiconductor/semiconductor grain boundaries before being injected into the oxide. In addition, as commented in the case of the dark voltammetry experiment, the aggregation of QDs in the external part of the channels forming part of the mesoporous structure blocks the access of sulfite to the interior of the channels, leading to full recombination. A similar behavior has been observed for TiO_2 electrodes sensitized with CdS[4,8] QDs prepared by successive ionic layer reaction and, in the case of CdSe,[27,44] prepared by chemical bath deposition. In such cases, the IPCE only increases for the first coatings, while, for the electrodes with a larger amount of semiconductor sensitizer, a strong decrease of the IPCE is observed. However, in these methods, both an increase in the number of QDs and an increase in the nanoparticle size simultaneously take place. As observed in Figure 6B, the maximum IPCE value at the excitonic peak wavelength is nearly 40%, evidencing efficient transfer of both electrons from CdSe toward TiO_2 and holes from CdSe toward sulfite.

When the IPCE measurements are repeated for the MPA-attached QDs, a different behavior is observed. In this case, an increase in adsorption time leads to an increase in the IPCE except for very large adsorption times. This can be simply explained by the fact that more light is harvested as the amount of QDs attached to the MPA linker increases. Seemingly, the expected lack of QD aggregation avoids now the drastic decrease of the IPCE observed in the case of direct adsorption. Probably, some degree of aggregation could exist for the longer adsorption time employed in the experiments. Figure 7A presents a plot of the IPCE versus the wavelength for the QD attachment via the molecular linker for different adsorption times, while Figure 7B corresponds to the IPCE vs 100-R/% both evaluated at the excitonic peak.

It is worth noting that for equivalent reflectance values (and roughly similar QD loading), the IPCE is much larger in the case of direct adsorption. For instance, for a 100-R/% value of 70%, the IPCE in the case of direct adsorption equals 35%, while a value lower than 2% was obtained when the MPA linker was employed. This clearly suggests that, when the QDs are directly attached to the surface, the electronic injection is favored. Probably, this mode of attachment involves a partial removal of the TOP layer at the points of contact with the oxide particles and, therefore, a minimization of the distance between the QD (electron donor) and the TiO_2 particle (electron acceptor). If the transfer occurs through tunneling, such a minimization is desirable and could explain the high IPCE as compared to that obtained with the MPA-mediated attachment. In such a case, the MPA linker would lead to a decrease of the IPCE. However, it should be mentioned that the molecular linker could also play a specific role in the electron transfer process as demonstrated by the 4-fold improvement in the IPCE observed when cysteine instead of MPA is used as a molecular linker.[25]

Conclusions

TiO_2 thin layer electrodes have been sensitized to the visible by incorporating 3.4 nm TOP-capped CdSe QDs in two different ways: by direct adsorption or via a molecular linker such as MPA. The results obtained in both cases and their comparison provide some ideas about the strategy to follow in order to improve the behavior of QD-sensitized photoanodes. A way to achieving the direct incorporation of the QDs in the TiO_2 nanoporous layer relies on a change in the solvent used to disperse the QDs. A favorable interaction of the QDs with both the solvent where they are dispersed and with the oxide surface would lead to a high degree of coverage with a low degree of aggregation. In our case, dispersing the TOP-capped CdSe QDs in CH_2Cl_2 leads to their fast attachment to the TiO_2 layer. However, it should be indicated that direct adsorption, as evidenced by AFM, leads to an important degree of QD aggregation, especially in the outermost part of the TiO_2 nanoporous layer.

Interestingly, by direct chemical analysis of the Cd contained in the TiO_2 film, a fractional coverage of only 0.14 is obtained at saturation (for both attachment modes), which is evidence that a major issue when using QD sensitizers is making most of the inner surface of the oxide nanostructure accessible to the QDs. An option is the use of films composed of adequately spaced oxide nanocolumns or nanorods, even when their inner surface is smaller than that of typical nanoparticulate films.

Detailed studies have been done on the dependence of the IPCE on QD coverage. In spite of the low fractional coverage attained, a value as high as 36% is obtained for the IPCE at the excitonic peak wavelength in the case of direct adsorption, much higher than in the case of MPA-mediated adsorption. This suggests that a direct contact (or close proximity) between the QDs and the oxide nanoparticle is beneficial for the efficiency of the photoanode. However, QD aggregation leads, for high QD coverages, to a severe drop in the IPCE, probably linked to the existence of QD−QD contacts, but also to a blockage of the TiO_2 film nanochannels by accumulation of QD aggregates. In contrast, for QDs attached via MPA, the IPCE monotonously increases with coverage. Further work is in progress to apply other methods for direct CdSe QD adsorption and to change the oxide nanostructure, making it more open.

Acknowledgment. This work was financially supported by the Spanish Ministry of Science and Innovation through projects HOPE CSD2007-00007(Consolider-Ingenio2010) and CTQ2006-06286. N.G. thanks the MEC for the award of a FPU grant.

Supporting Information Available: Kubelka−Munk transformation of the reflectance spectra for the QD-sensitized TiO_2 thin films and cadmium concentration versus 100-Reflectance(%) plot for TiO_2 nanoporous films sensitized with CdSe QDs. This material is available free of charge via the Internet at http://pubs.acs.org.

References and Notes

(1) O'Regan, B.; Grätzel, M. *Nature* **1991**, *353*, 737–740.
(2) Nozik, A. J. *Physica E* **2002**, *14*, 115–120.
(3) Nozik, A. J. *Chem. Phys. Lett.* **2008**, *457*, 3–11.
(4) Vogel, R.; Pohl, K.; Weller, H. *Chem. Phys. Lett.* **1990**, *174*, 241–246.
(5) Vogel, R.; Hoyer, P.; Weller, H. *J. Phys. Chem.* **1994**, *98*, 3183–3188.
(6) Qian, X.; Qin, D.; Bai, Y.; Li, T.; Tang, X.; Wang, E.; Dong, S. *J. Solid State Electrochem.* **2001**, *5*, 562–567.
(7) Peter, L. M.; Riley, D. J.; Tull, E. J.; Wijayantha, G. U. *Chem.Commun.* **2002**, 1030–1031.
(8) Toyoda, T.; Sato, J.; Shen, Q. *Rev. Sci. Instrum.* **2003**, *74*, 297–299.
(9) Tachibana, Y.; Umekita, K.; Otsuka, Y.; Kuwabata, S. *J. Phys. D: Appl. Phys.* **2008**, *41*, 102002.
(10) Shen, Y.-J.; Lee, Y.-L. *Nanotechnology* **2008**, *19*, 045602.
(11) Hoyer, P.; Koenenkamp, R. *Appl. Phys. Lett.* **1995**, *66*, 349–351.
(12) Hong, J. S.; Choi, D. S.; Kang, M. G.; Kim, D.; Kim, K.-J. *J. Photochem. Photobiol. A* **2001**, *143*, 87–92.
(13) Plass, R.; Pelet, S.; Krueger, J.; Graetzel, M.; Bach, U. *J. Phys. Chem. B* **2002**, *106*, 7578–7580.
(14) Zaban, A.; Micic, O. I.; Gregg, B. A.; Nozik, A. J. *Langmuir* **1998**, *14*, 3153–3156.
(15) Yu, P.; Zhu, K.; Norman, A. G.; Ferrere, S.; Frank, A. J.; Nozik, A. J. *J. Phys. Chem. B* **2006**, *110*, 25451–25454.
(16) Liu, D.; Kamat, P. V. *J. Phys. Chem.* **1993**, *97*, 10769–10773.
(17) Fang, J.; Wu, J.; Lu, X.; Shen, Y.; Lu, Z. *Chem. Phys. Lett.* **1997**, *270*, 145–151.
(18) Shen, Q.; Arae, D.; Toyoda, T. *J. Photochem. Photobiol. A* **2004**, *164*, 75–80.
(19) Shen, Q.; Katayama, K.; Yamaguchi, M.; Sawada, T.; Toyoda, T. *Thin Solid Films* **2005**, *486*, 15–19.
(20) Robel, I.; Subramanian, V.; Kuno, M.; Kamat, P. V. *J. Am. Chem. Soc.* **2006**, *128*, 2385–2393.
(21) Shen, Q.; Sato, T.; Hashimoto, M.; Chen, C.; Toyoda, T. *Thin Solid Films* **2006**, *499*, 299–305.
(22) Niitsoo, O.; Sarkar, S. K.; Pejoux, C.; Ruehle, S.; Cahen, D.; Hodes, G. *J. Photochem. Photobiol. A* **2006**, *181*, 306–313.
(23) Diguna, L. J.; Shen, Q.; Kobayashi, J.; Toyoda, T. *Appl. Phys. Lett.* **2007**, *91*, 023116.
(24) Kongkanand, A.; Tvrdy, K.; Takechi, K.; Kuno, M.; Kamat, P. V. *J. Am. Chem. Soc.* **2008**, *130*, 4007–4015.
(25) Mora-Seró, I.; Giménez, S.; Moehl, T.; Fabregat-Santiago, F.; Lana-Villarreal, T.; Gómez, R.; Bisquert, J. *Nanotechnology* **2008**, *19*, 424007.
(26) Lee, H. J.; Kim, D.-Y.; Yoo, J.-S.; Bang, J.; Kim, S.; Park, S.-M. *Bull. Korean Chem. Soc.* **2007**, *28*, 953–958.
(27) Shen, Q.; Kobayashi, J.; Diguna, L. J.; Toyoda, T. *J. Appl. Phys.* **2008**, *103*, 084304.
(28) López-Luke, T.; Wolcott, A.; Xu, L.-P.; Chen, S.; Wen, Z.; Li, J.; de la Rosa, E.; Zhang, J. Z. *J. Phys. Chem. C* **2008**, *112*, 1282–1292.
(29) Wang, Q.; Pan, D.; Jiang, S.; Ji, X.; An, L.; Jiang, B. *J. Cryst. Growth* **2006**, *286*, 83–90.
(30) Nakamura, R.; Ohashi, N.; Imanisi, A.; Osawa, T.; Matsumoto, Y.; Koinuma, H.; Nakato, Y. *J. Phys. Chem. B* **2005**, *109*, 1648–1651.
(31) Yu, W. W.; Qu, L. H.; Guo, W. Z.; Peng, X. G. *Chem. Mater.* **2003**, *15*, 2854–2860.
(32) Sarkar, S. K.; Hodes, G. *J. Phys. Chem. B* **2005**, *109*, 7214–7219.
(33) Leatherdale, C. A.; Bawendi, M. G. *Phys. Rev. B* **2001**, *63*, 165315.
(34) Koole, R.; Luigjes, B.; Tachiya, M.; Pool, R.; Vlugt, T. J. H.; de Mello Donegá, C.; Meijerink, A.; Vanmaekelbergh, D. *J. Phys. Chem. B* **2007**, *111*, 11208–11215.
(35) Berger, T.; Lana-Villarreal, T.; Monllor-Satoca, D.; Gómez, R. *Electrochem. Commun.* **2006**, *8*, 1713–18.
(36) Lee, J. L.; Yum, J.-H.; Leventis, H. C.; Zakeeruddin, S. M.; Haque, S. A.; Chen, P.; Seok, S. I.; Grätzel, M.; Nazeeruddin, M. K. *J. Phys. Chem. C* **2008**, *112*, 11600.
(37) Fabregat-Santiago, F.; Mora-Seró, I.; Garcia-Belmonte, G.; Bisquert, J. *J. Phys. Chem. B* **2003**, *107*, 758–768.
(38) Bisquert, J.; Fabregat-Santiago, F.; Mora-Seró, I.; Garcia-Belmonte, G.; Barea, E. M.; Palomares, E. *Inorg. Chim. Acta* **2008**, *361*, 684–698.
(39) Berger, T.; Lana-Villarreal, T.; Monllor-Satoca, D.; Gómez, R. *J. Phys. Chem. C* **2007**, *111*, 9936–9942.
(40) De La Garza, L.; Saponjic, Z. V.; Dimitrijevic, N. M.; Thurnauer, M. C.; Rajh, T. *J. Phys. Chem. B* **2006**, *110*, 680–686.
(41) Neale, N. R.; Kopidakis, N.; van de Lagemaat, J.; Grätzel, M.; Frank, A. J. *J. Phys. Chem. B* **2005**, *109*, 23183–23189.
(42) Zhang, Z.; Zakeeruddin, S. M.; O'Regan, B. C.; Humphry-Baker, R.; Grätzel, M. *J. Phys. Chem. B* **2005**, *109*, 21818–21824.
(43) Rühle, S.; Greenshtein, M.; Chen, S.-G.; Merson, A.; Pizem, H.; Sukenik, C. S.; Cahen, D.; Zaban, A. *J. Phys. Chem. B* **2005**, 18907–18913.
(44) Toyoda, T.; Kobayashi, J.; Shen, Q. *Thin Solid Films* **2008**, *516*, 2426–2431.

JP808091D